STRUCTURAL DYNAMICS OF SOLID PROPELLANTS WITH FREQUENCY DEPENDENT PROPERTIES

N. Merlette [(1)], E. Pagnacco [(2)]

[(1)] TANGENT'DELTA, 1 rue Adolphe Robert – 58200 Cosne Cours sur Loire (France), Email:nicolas.merlette@tgdelta.com
[(2)] Laboratoire de Mécanique de Rouen, INSA de Rouen, Avenue de l'Université – 76800 Saint Etienne du Rouvray (France), Email:emmanuel.pagnacco@insa-rouen.fr

ABSTRACT

This paper addresses the dynamic behaviour of solid propellants as linear viscoelastic materials with frequency dependent mechanical properties. Experimental data of a typical propellant are used to highlight the frequency dependence of the storage modulus and the loss factor. This phenomenon is then tackled in a transient analysis of a Ariane-5 booster-like stage. Finite element computations are performed with Code_Aster and dedicated user developments. Results are compared with a constant elastic approach, in order to show the influence of the frequency dependence on the structural dynamics of the booster-like stage.

1. INTRODUCTION

Solid propellants are energy materials used for space propulsion systems. The chemical reaction of decomposition of the propellant gives rise to the release of large amounts of energy and hot gases in the rocket motor. The gases are then channelled through the converging nozzle to create the propulsive effect. It is well known that this combustion is a source of transient mechanical excitations for the rocket structure and the embedded satellites.

Because of their complex behaviour and the difficulty to characterize their dynamic properties, solid propellants are often simplified as elastic materials with constant properties in finite element models of space propulsion systems. This simplification may lead to inaccurate results in the prediction of structural dynamics of solid propellants.

The first part of this paper addresses the viscoelasticity of solid propellants. The frequency dependence of their dynamic behaviour is highlighted using data of a typical Hydroxyl-Terminated PolyButadiene (HTPB) propellant.

The second part tackles this phenomenon in the case of a transient analysis of a solid booster-like stage. The propellant is modelled as a viscoelastic material with frequency dependent storage modulus and loss factor. The finite element analysis is performed with Code_Aster. Results are compared with the conventional elastic model.

2. DYNAMIC BEHAVIOUR OF SOLID PROPELLANTS

2.1. Viscoelastic material

Solid propellants have a complex mechanical behaviour, usually described as nonlinear hyper-viscoelastic. Strong hysteresis can be observed when propellant samples are tested in tension-relaxation cycles. Viscous effects within the material are responsible for this phenomenon, which is dependent on the velocity of the strain. In addition to the viscoelasticity, the heterogeneity of the microstructure is responsible for both physical and geometrical nonlinearities, depending on the operating conditions. As an example, the dynamic behaviour of a Butalane® propellant was observed as nonlinear in relation to the amplitude of the strain and to the rate of the static pre-stress [1]. The development of a behaviour law taking into account all the nonlinearities is still a challenge.

In this work, the nonlinearities of the dynamic behaviour are not addressed. The solid propellant is considered as a linear viscoelastic material, in order to enhance the damping effects by comparing with the classical linear elastic model.

2.2. Complex modulus representation

Like polymers, the complex modulus representation [2] can be used to take into account the linear viscoelastic behaviour of solid propellants in finite element computations. Indeed, the behaviour of a propellant working in tension-compression can be represented by only two of the three parameters, namely the storage modulus E', the loss modulus E'' and the loss factor η_E. Thus, the complex Young's modulus can be written as:

$$E^* = E' + iE'' = E'\left(1 + i\eta_E\right), \qquad (1)$$

with:

$$\eta_E = \frac{E''}{E'}. \qquad (2)$$

For a propellant working in shear, Eq. 1 can be rewritten

for the complex shear modulus as follows:

$$G^* = G' + iG'' = G'\left(1 + i\eta_G\right), \tag{3}$$

with:

$$\eta_G = \frac{G''}{G'}. \tag{4}$$

Depending on the use of a propellant, it can be deformed either in pure tension-compression or in pure shear as depicted in Fig. 1. It is often a combination of both when propellant combustion excites a complex structure in a large dynamic range.

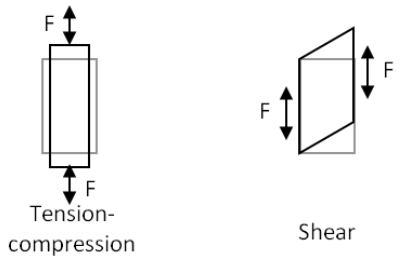

Figure 1. Tension-compression and shear deformation.

For a truly isotropic material, the Young's and shear moduli are related by the Poisson's ratio ν, according to the classical theory:

$$G' = \frac{E'}{2\left(1+\nu\right)}. \tag{5}$$

The loss factor is then supposed to be unique:

$$\eta = \eta_E = \eta_G. \tag{6}$$

Unfortunately, as for many viscoelastic materials, E' and G' may not satisfy the isotropic conditions of Eq. 5 using acceptable values of ν (close to 0.5). Moreover, the loss factors η_E and η_G may also differ significantly.
To emphasize, only the isotropic viscoelastic behaviour of propellants will be addressed, but what follows can be extended to anisotropic behaviours.

2.3. Frequency dependence

In practice, the dynamic behaviour of solid propellants varies with environmental factors as humidity, pressure, temperature and frequency. Temperature and frequency are usually considered as the most important factors affecting the properties of viscoelastic materials. For many of them, stiffness will increase with frequency, whereas it will decrease with temperature. To take into account these temperature and frequency dependences in finite element computations, Eq. (1) is rewritten as:

$$E^*(\omega,T) = E'(\omega,T)\left[1 + i\eta_E(\omega,T)\right], \tag{7}$$

where the two functions of frequency and temperature can be obtained from dynamic characterizations or fitted with analytical functions from rheological models. Dynamic Mechanical Analysis (DMA) can provide tabulated values of the two functions directly from tension-compression tests of propellant samples. DMA data of a typical HTPB propellant tested in tension-compression [3] are presented in Fig. 2 in the form of the so-called "wicket plot" where the loss factor is plotted as a function of the storage modulus.

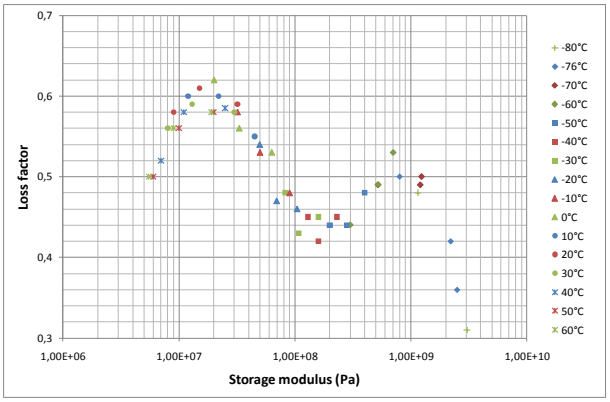

Figure 2. Wicket plot of the loss factor in function of the storage modulus for a HTPB propellant [3].

One sample of the HTPB propellant was tested for three frequencies (7.8 Hz, 31.3 Hz and 125 Hz) and for a temperature range between -80°C and +60°C. The curve presented in Fig. 2 has the form of an inverse ω-shape. The first peak is characteristic of the free macromolecules displacements in the elastomeric network, whereas the second one is attributed to the glass transition around -70°C.

As the effect of frequency on the dynamic properties is the inverse of that of temperature, the complex modulus of a viscoelastic material is classically described using only one parameter: the reduced frequency. It has been demonstrated [4] the theory of the frequency/temperature equivalence can be used to determine the complex modulus of a solid propellant as a function of the reduced frequency. From the DMA data of the HTPB propellant, the master curve of the storage modulus was built up and the shift factors, $\log\left(a_T\right)$, were derived via the Williams-Landel-Ferry equation:

$$\log\left(a_T\right) = \frac{-C_1\left(T - T_{ref}\right)}{C_2 + T - T_{ref}}, \tag{8}$$

where T_{ref} is the reference temperature chosen to build up the master curve and C_1 and C_2 are constants adjusted to fit the values of a_T. The reduced frequencies are then obtained by multiplying the measured frequencies with the corresponding values of a_T. As a result, the storage modulus and the loss factor of the HTPB propellant are given in Fig. 3 as functions of the reduced frequency for the reference temperature of 20°C.

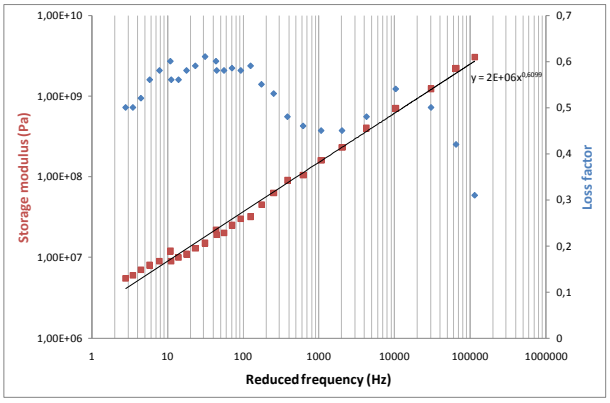

Figure 3. Master curves of storage modulus and loss factor for a HTPB propellant at the reference temperature of 20°C [3].

It is clear the dynamic properties of the HTPB propellant are strongly frequency dependent. The values of the storage modulus and the loss factor vary respectively between 5.5 and 3050 MPa and between 0.31 and 0.61 in all the frequency range. The storage modulus raises in function of the frequency, whereas the loss factor presents two main peaks around 30 Hz (0.61) and 10000 Hz (0.54) and a valley between 1000 and 2000 Hz.

3. TRANSIENT ANALYSIS OF A SOLID BOOSTER-LIKE STAGE

A finite element analysis of a Ariane-5 booster-like stage's rocket motor loading with a solid propellant was performed. The aim was to study the influence of the frequency dependence of the mechanical properties of the propellant on the global dynamic behaviour of the booster stage.

3.1. Description of the model

A finite element model was built using the software Salome with the objective to represent the macro mechanical behaviour of a Ariane-5 booster-like stage. The mesh consists in 9284 shell elements for the structure of the booster stage, 13500 solid elements for the propellant and a few beam elements for the attachment ring and the connecting rods with the Ariane-5 central stage. Shell and solid elements were linked with coincident nodes (compatible meshes). The ends of the connecting rods were clamped as boundary conditions of the booster stage. The resulting mesh is presented in Fig. 4.

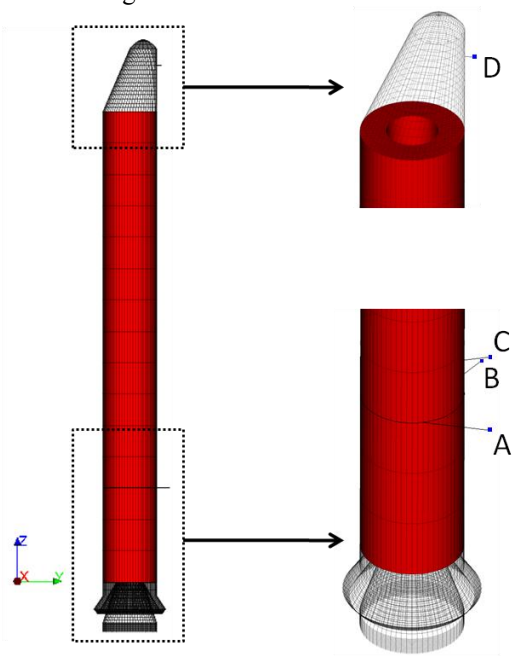

Figure 4. Finite element mesh of the solid booster stage. Propellant with solid elements in red. Clamping conditions at nodes A, B, C and D.

The mesh of the propellant was realized as a hollow cylinder with fifteen layers in the thickness. Using a density of 1713 kg/m³, it represents a total load of 238 tons of solid propellant. Taking into account the clamping conditions at nodes A, B, C and D, the total number of active degrees of freedom was 93150.

3.2. Computing methodology

The objective was to compute transient responses of the booster stage for an impulse excitation simulating the rupture of the propellant tank diaphragm. A Ricker-like impulse signal was tuned in order to excite the vibratory modes of the booster stage only between 0 and 300 Hz. The resulting excitation force is presented in Fig. 5 in time-domain up to 0.2 seconds. The total time of the signal is 10 seconds.

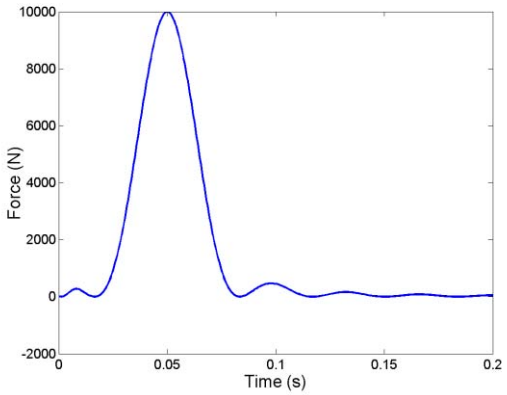

Figure 5. Excitation force of the booster stage in time-domain.

The excitation force is also given in Fig. 6 in the frequency domain.

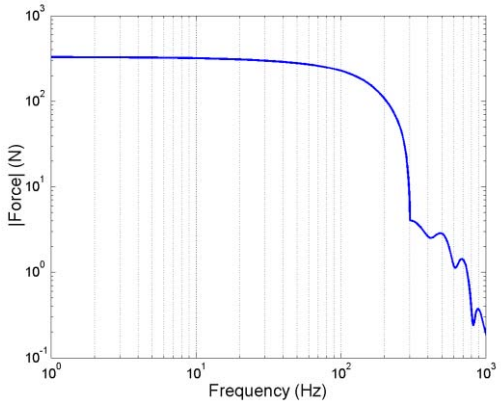

Figure 6. Excitation force of the booster stage in frequency domain.

The excitation force was then distributed among all the nodes on the perimeter of the diaphragm.

The transient response of the structure corresponds to a convolution product in time-domain, which is easier to evaluate in the frequency domain. Therefore, in order to take into account the frequency dependence of the mechanical properties of the propellant, the following procedure was performed. First, harmonic responses were computed via a direct approach solving:

$$\{U(\omega)\} = \left(\left[K^*(\omega)\right] - \omega^2[M]\right)^{-1}\{F(\omega)\}, \qquad (9)$$

for all the frequency steps between 0 and 1000 Hz. The complex stiffness matrix of the system, $[K^*(\omega)]$, was realized for each frequency step as:

$$[K^*(\omega)] = [K_e^*] + [K_v^*(\omega)], \qquad (10)$$

where $[K_e^*]$ is a constant complex stiffness matrix representing the elastic parts of the booster structure and $[K_v^*(\omega)]$ is a frequency dependent complex stiffness matrix representing the propellant as a linear viscoelastic material. Using the master curves of the HTPB propellant presented in Fig. 3, $[K_v^*(\omega)]$ was realized for each frequency step as:

$$[K_v^*(\omega)] = \frac{E'(\omega)}{E'_{ref}}[K_{ref}]\left(1 + i\eta(\omega)\right), \qquad (11)$$

with E'_{ref}, a reference storage modulus which was defined for a reference frequency, ω_{ref}, selected within the frequency range. The reference real stiffness matrix, $[K_{ref}]$, was extracted from the global real stiffness matrix of the system for the reference storage modulus using a "double assembly" procedure [5] as:

$$[K_{ref}] = [K(2E'_{ref})] - [K(E'_{ref})]. \qquad (12)$$

Second, reaction forces were derived from the computed harmonic responses at the four clamping conditions. Each reaction force was calculated as the component normal to the beam section at the clamped node (A, B, C, or D). Finally, reaction forces were returned in time-domain via an inverse Fast Fourier Transform.

In addition, reaction forces were also computed for constant mechanical properties of the propellant repeating the procedure described above. Values at 50 Hz were used for the storage modulus and the loss factor. In this case, the complex stiffness matrix of Eq. 9 was realized only once.

Computations were realized with the finite element code Code_Aster. Some user developments were added to define a frequency dependent viscoelastic material and to compute harmonic responses with realization of the stiffness matrix at each frequency step.

3.3. Results

Fig. 7 to Fig. 10 compare in time-domain up to 5 seconds the results obtained with and without frequency dependence for the four nodes where the reaction forces were computed.

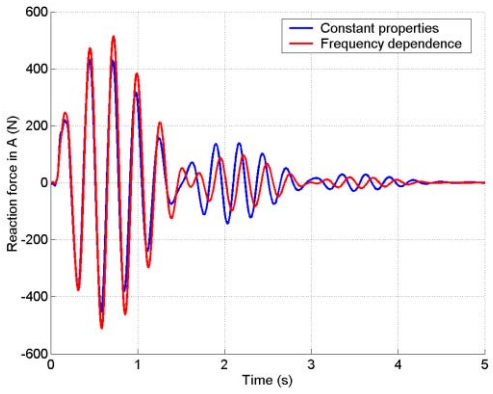

Figure 7. Comparison in time-domain of the reaction forces computed at node A with and without frequency dependence.

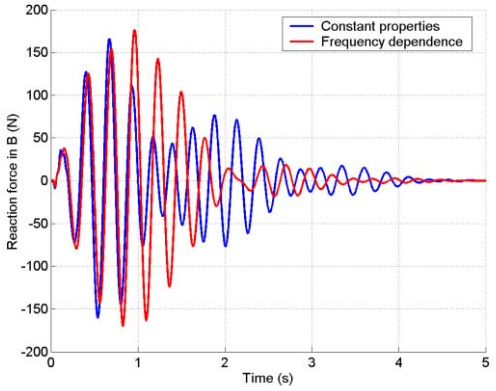

Figure 8. Comparison in time-domain of the reaction forces computed at node B with and without frequency dependence.

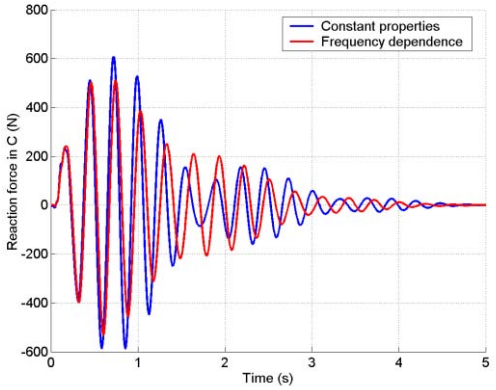

Figure 9. Comparison in time-domain of the reaction forces computed at node C with and without frequency dependence.

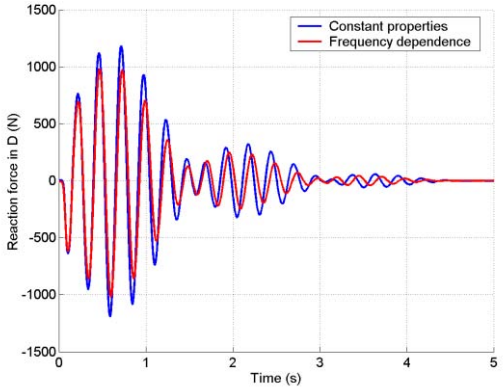

Figure 10. Comparison in time-domain of the reaction forces computed at node D with and without frequency dependence.

Differences in amplitude and time delays are clearly observed for the four nodes when frequency dependent properties of the propellant are taken into account or not. Amplitudes vary up to 200 N (2% of the maximum excitation level) for the node D in the upper part of the booster stage, where the highest levels of the reaction forces were computed. Shapes of the transient signals are much more different for the node B in the lower part of the booster stage. These differences are confirmed in frequency domain by comparing the reaction force spectra between 1 and 200 Hz in Fig. 11 to Fig. 14.

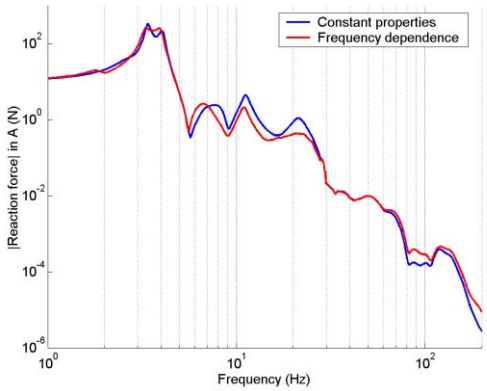

Figure 11. Comparison in frequency domain of the reaction forces computed at node A with and without frequency dependence.

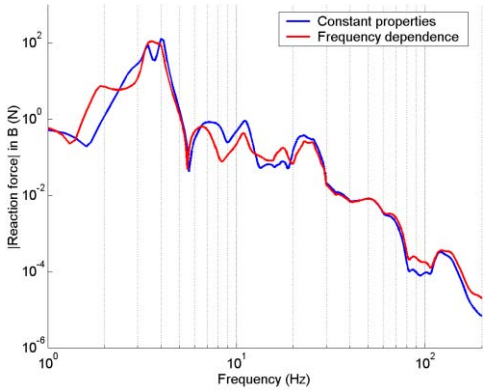

Figure 12. Comparison in frequency domain of the reaction forces computed at node B with and without frequency dependence.

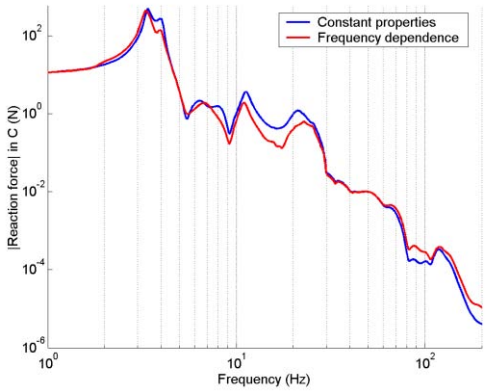

Figure 13. Comparison in frequency domain of the reaction forces computed at node C with and without frequency dependence.

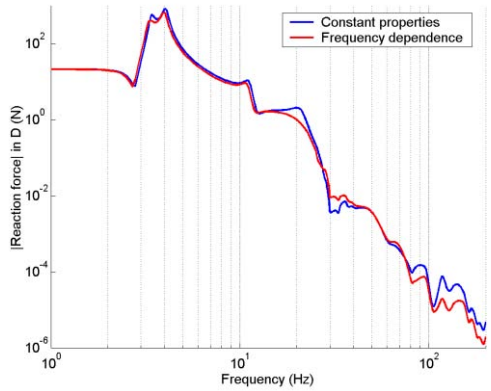

Figure 14. Comparison in frequency domain of the reaction forces computed at node D with and without frequency dependence.

Reaction forces computed with and without frequency dependence are different in all the frequency range of interest, except at the frequency of 50 Hz for which the stiffness matrix of the constant approach was realized. Before 5 Hz, important differences in shapes and levels are observed for node B, whereas they are less visible for the other three nodes. This modification of the low frequency dynamics of the booster stage can explain why the shapes of the two transient signals computed for node B are so different. Regarding the amplitudes, the maximum difference is for node D again with a reduction of 200 N for the peak at 4 Hz, when frequency dependent properties of the propellant are taken into account.

Finally, it has been demonstrated that an error in the realization of the real stiffness matrix will lead to errors in the periods of the oscillations. In addition, an error in the damping of the structure will change the levels of the oscillations. But the combination of both errors may be a stronger problem, because it may lead to compute wrong phases and wrong modal contributions. This problem is visible for the first oscillation in Fig. 7 and Fig. 8.

4. CONCLUSION

The dynamic behaviour of solid propellants has been addressed with the objective to perform finite element analyses. They have been considered as viscoelastic materials, in order to enhance the damping effects by comparing with the classical linear elastic model. The frequency dependence of their mechanical properties has been highlighted using DMA data of a typical HTPB propellant. It has been shown the storage modulus and the loss factor of the HTPB propellant are strongly frequency dependent.

A transient analysis of a booster-like stage was carried out to demonstrate the importance to take into account the frequency dependence of the propellant properties in structural dynamics of the global structure. A methodology has been proposed for transient responses computations of a booster-like stage comprising a frequency dependent viscoelastic propellant. The procedure was performed using Code_Aster with dedicated user developments. Comparing with the conventional constant approach, differences in responses have been discussed in time-domain and frequency domain.

5. ACKNOWLEDMENTS

The authors would like to thank Mr Germès S. for his general advices about dynamics of a solid booster stage.

6. REFERENCES

1. Azoug, A. (2010). Micromécanismes et comportement macroscopique d'un élastomère fortement chargé. PhD thesis pp. 91-94, Ecole Polytechnique ParisTech, France.

2. Nashif, A.D., Jones, D.I.G. & Henderson, J.P. (1985). *Vibration Damping*, John Wiley and Sons.

3. Nevière, R. , Lucas, M. (2003). Aging Properties of An HTPB Propellant. Final Report SPC 01-4072. Approved for Public Release. SNPE, France.

4. Nevière, R. (2006). An extension of the time-temperature superposition principle to non-linear viscoelastic solids. *International Journal of Solids and Structures* **43**, 5295–5306.

5. Abbadi, Z., Merlette, N., Roy, N. (2008). Response Computation of Structures with Viscoelastic Damping Materials using a Modal Approach - Description of the Method and Application on a Car Door Model Treated with High Damping Foam. In Proc. 5th Symposium on Automobile Comfort, Le Mans, France.